Heater Sizing Overview

Excel Sheet/Hand Calculation Basis:

With a known filament diameter, total mass, density, and time to produce the mass, a mass flow rate was established. With the geometric properties of the extruder barrel and auger screw known/selected, a volume in which material could occupy inside of the extruder was computed. Assuming equal density of the material inside the extruder as the filament strand, the velocity of the fluid inside of the extruder barrel was computed using conservation of mass. With known geometry of the extruder barrel and auger screw (average cross-sectional area for material flow and length of extrusion known), an average velocity was also computed.

With known values for the specific heat capacity for the material as a solid and a liquid, its melting temperature, its latent heat of fusion, inlet temperature, exit temperature, and total mass of material inside of the extruder at any point in time, the energy required to bring the material from the inlet temperature to the exit temperature was computed. With a known distance of the extruder and the velocity of the fluid, an increment of time in which the energy had to be inputted into the fluid was known, resulting in a known rate of heat transfer required. Losses due to convection from the surface of the extruder were estimated and added to the rate of heat transfer required.

The parameters (material properties and geometries excluded for brevity) were as follows:

- Filament diameter of 1.75mm
- Total filament mass of 1kg
- 1hr to produce the total mass of filament
- Extruder inlet temperature of 20C
- Extruder outlet Temperature of 350C
- Convective heat transfer coefficient of 10W/m^2*k
- Ambient air temperature of 20C
- Average extruder barrel temperature of 250C (overestimated to account for radiation)

This resulted in a required heat input rate of 318W.

Solidworks CFD Simulation:

A Solidworks CFD simulation was used in order to confirm the energy balance results obtained.

The parameters of the simulation consisted of the following:

- Inlet temperature of 20C
- Inlet mass flow rate equivalent to hand calcs determined
- Outlet pressure of 101kpa (ambient environment)
- Equivalent heat transfer coefficient at exterior of extruding barrel as hand calculations/energy balance method

- LDPE Non-Newtonian fluid (most comparable to HDPE used in energy balance method, note that PET was also considered, and similar results were obtained, but will not be covered in this overview)
- Surface roughness of 0.4 Ra (vendor supplied value)
- Solid material consisted of 321 stainless steel (vendor specified)

The physical model consisted of the following (all pertaining to the vendor supplied extruder barrel):

- A nozzle was added
- The section of the barrel that would be entirely occupied by the auger screw from the material input location to the motor side (opposite extrusion end) was solidified with an extrusion
- A relatively short tube with a diameter equivalent to that of the extruded filament was added after the nozzle to ensure no vortices were generated at the opening
- A solid extrusion was generated down the centerline of the barrel with a diameter such that the average cross-sectional area for fluid flow computed in the energy balance method was maintained
- 3 surfaces were specified for heating element locations based on considered band heaters

Figures 1-5 indicate the parameters used for the CFD computation.

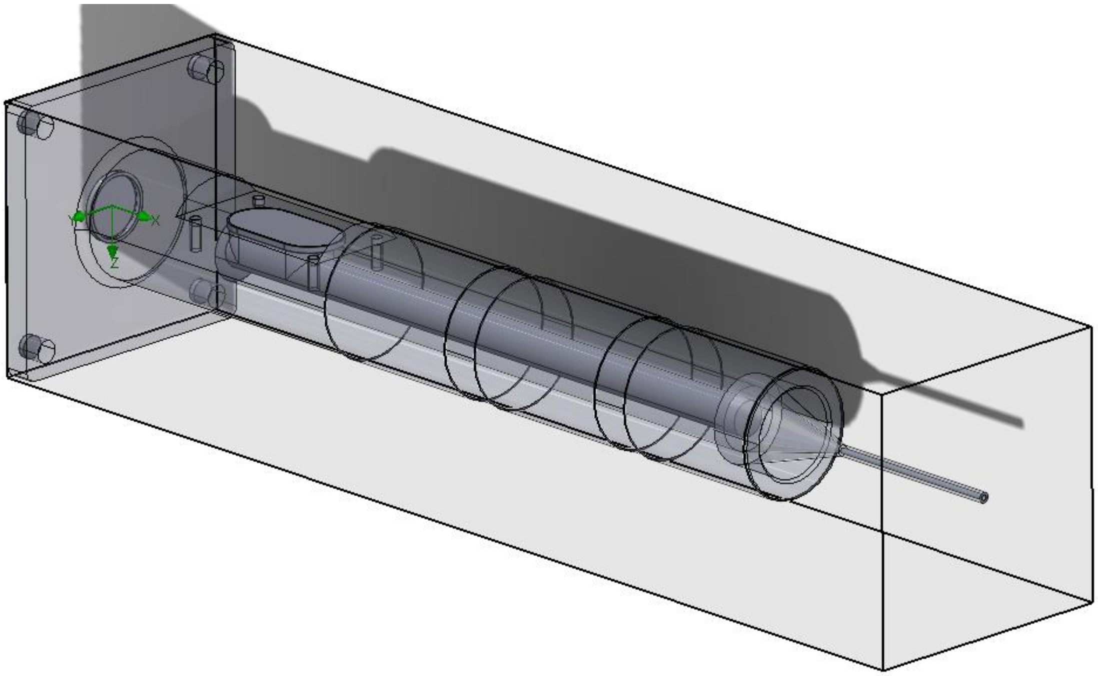

Figure 1: Computational Domain

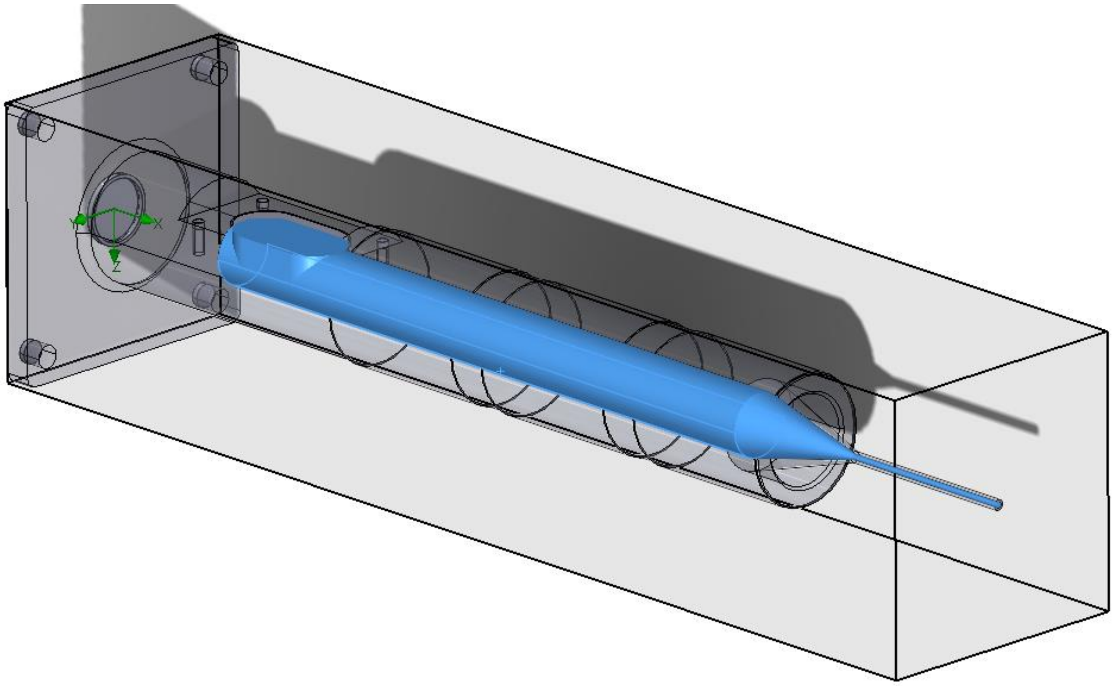

Figure 2: Fluid Domain

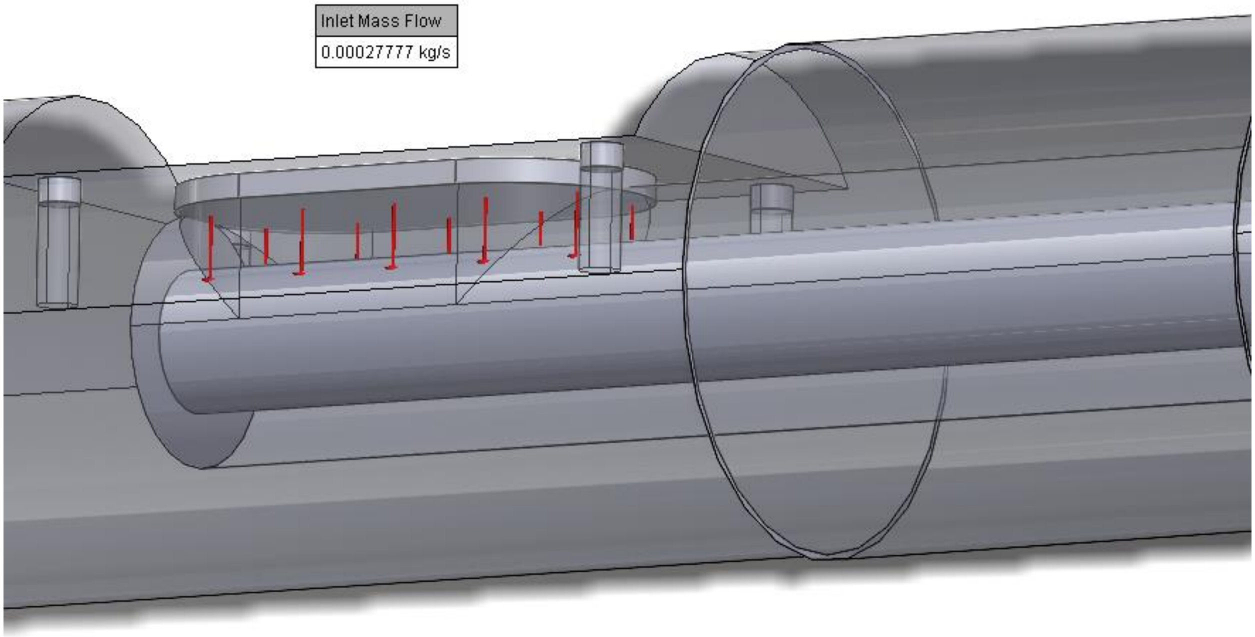

Figure 3: Inlet Condition

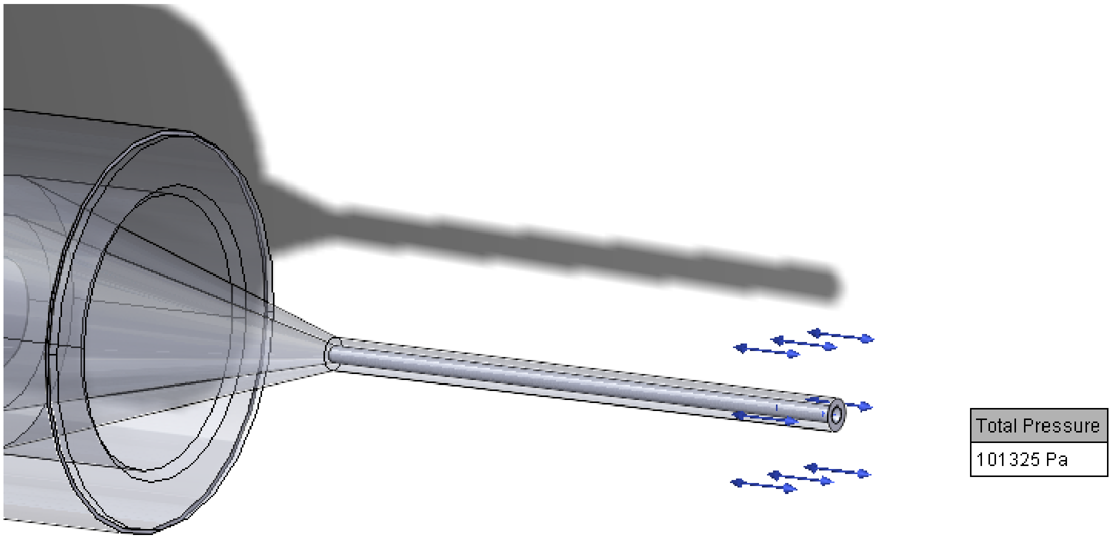

Figure 4: Outlet Condition

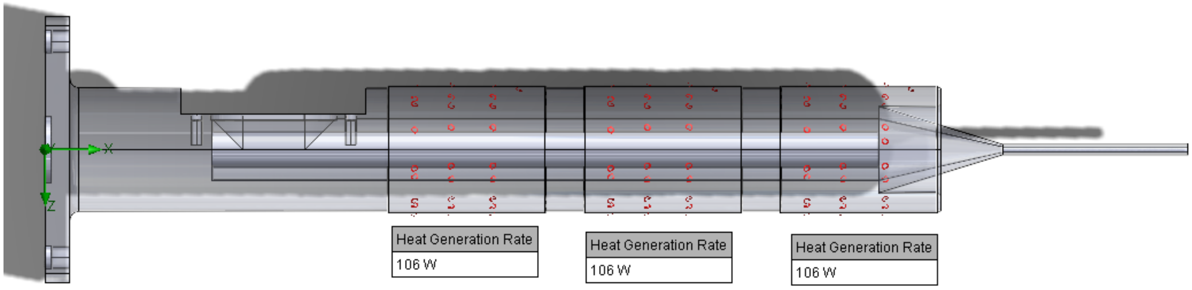

Figure 5: Heat Input Conditions

Note that these conditions are equivalent to those determined and specified in the energy balance method.

Next, it was ensured that the results obtained were independent of mesh size by considering two different mesh resolutions for equivalent inputs. In Solidworks, there is a scale from 1-7 that can be used to control the coarseness of the mesh used, with 7 being the most fine (smallest elements). There are also manual options available but using the built in mesh tool is typically the best choice, as there are mesh verification methods implemented in the software.

A refinement level of 4 and 7 were selected, Figures 6-12 indicate these results.

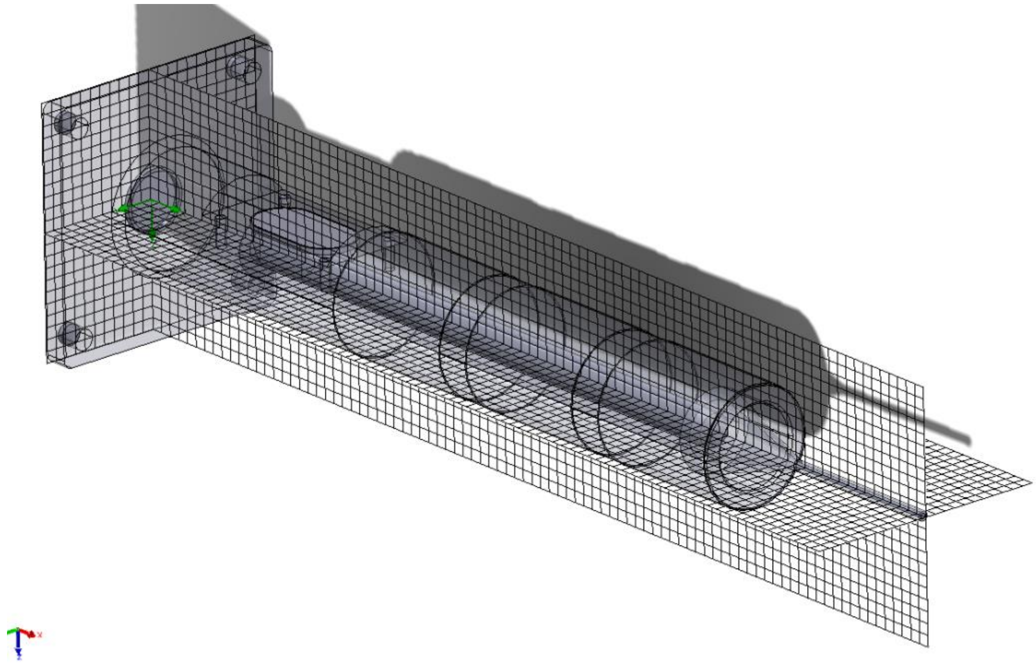

Figure 6: Mesh Refinement Level of 4

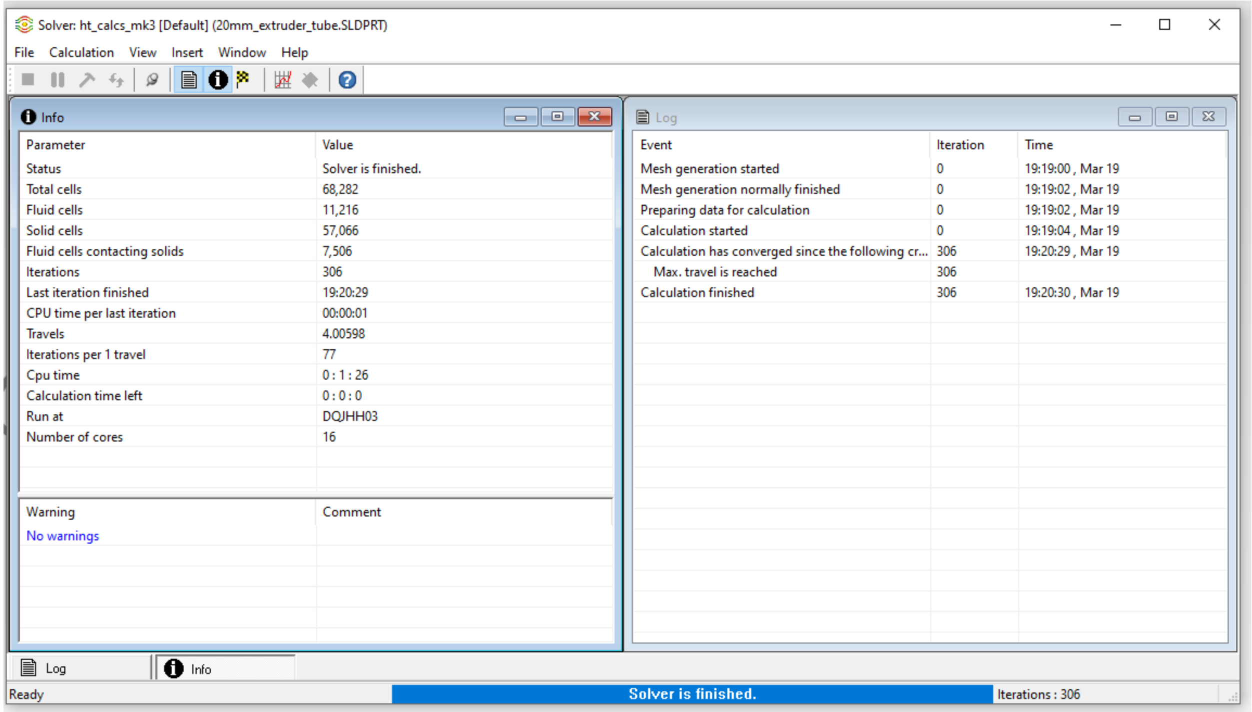

Parameter	Value
Status	Solver is finished.
Total cells	68,282
Fluid cells	11,216
Solid cells	57,066
Fluid cells contacting solids	7,506
Iterations	306
Last iteration finished	19:20:29
CPU time per last iteration	00:00:01
Travels	4.00598
Iterations per 1 travel	77
Cpu time	0 : 1 : 26
Calculation time left	0 : 0 : 0
Run at	DQJHH03
Number of cores	16

Warning	Comment
No warnings	

Event	Iteration	Time
Mesh generation started	0	19:19:00 , Mar 19
Mesh generation normally finished	0	19:19:02 , Mar 19
Preparing data for calculation	0	19:19:02 , Mar 19
Calculation started	0	19:19:04 , Mar 19
Calculation has converged since the following cr...	306	19:20:29 , Mar 19
Max. travel is reached	306	
Calculation finished	306	19:20:30 , Mar 19

Ready

Solver is finished.

Iterations : 306

Figure 7: Mesh Refinement Level of 4, Solver Window

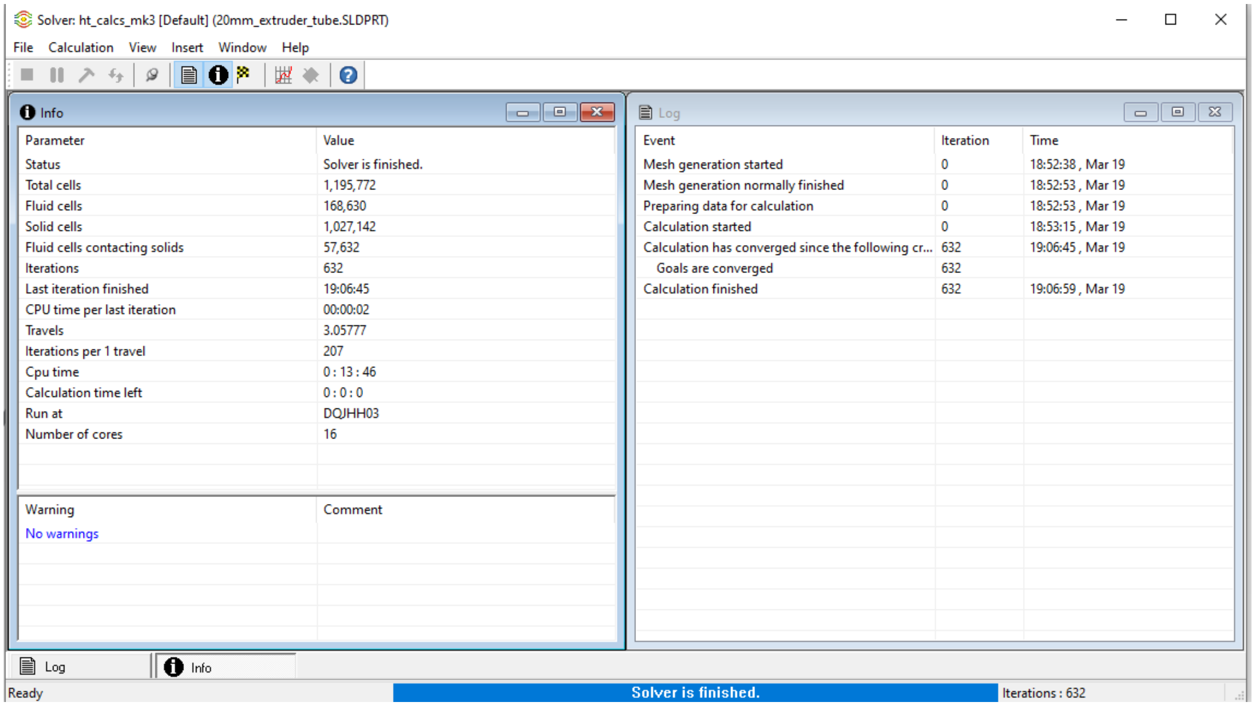

Parameter	Value
Status	Solver is finished.
Total cells	1,195,772
Fluid cells	168,630
Solid cells	1,027,142
Fluid cells contacting solids	57,632
Iterations	632
Last iteration finished	19:06:45
CPU time per last iteration	00:00:02
Travels	3.05777
Iterations per 1 travel	207
Cpu time	0 : 13 : 46
Calculation time left	0 : 0 : 0
Run at	DQJHH03
Number of cores	16

Warning	Comment
No warnings	

Event	Iteration	Time
Mesh generation started	0	18:52:38 , Mar 19
Mesh generation normally finished	0	18:52:53 , Mar 19
Preparing data for calculation	0	18:52:53 , Mar 19
Calculation started	0	18:53:15 , Mar 19
Calculation has converged since the following cr...	632	19:06:45 , Mar 19
Goals are converged	632	
Calculation finished	632	19:06:59 , Mar 19

Ready
Solver is finished.
Iterations : 632

Figure 8: Mesh Refinement Level of 7, Solver Window

Note the differences between the number of elements considered and the computation time.

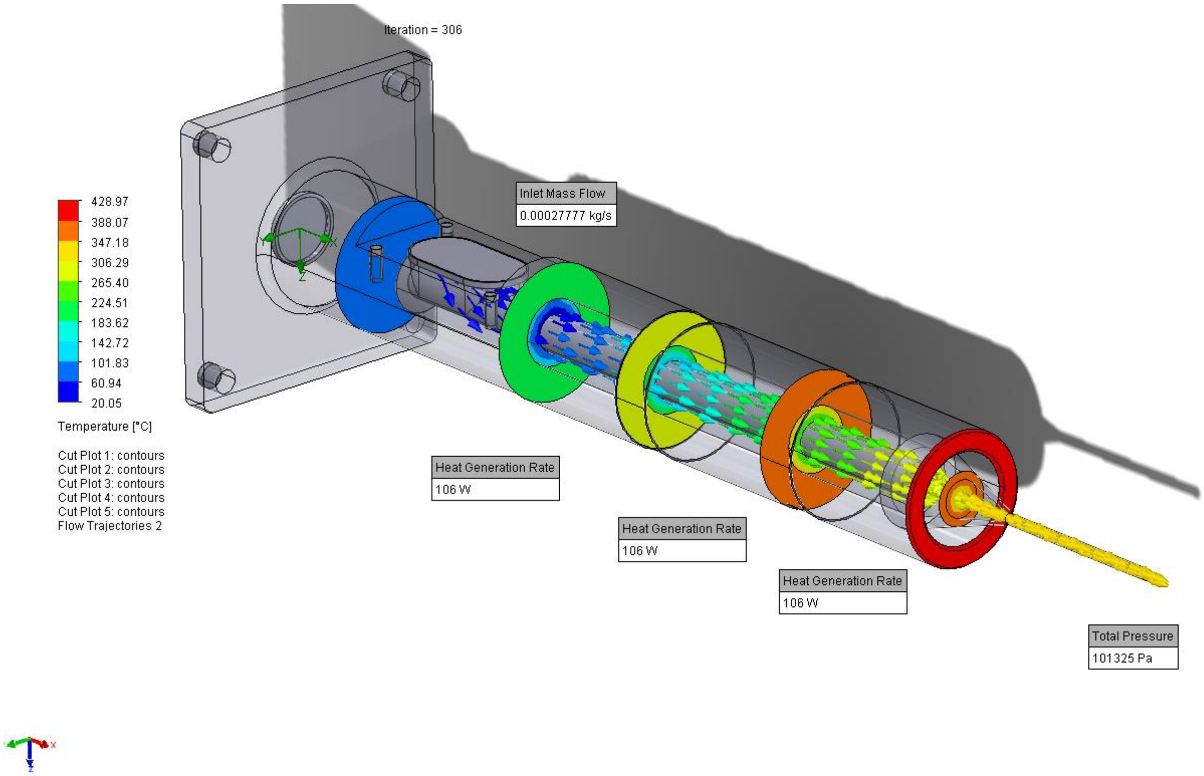

Figure 9: Mesh Refinement of 4, Overall Results

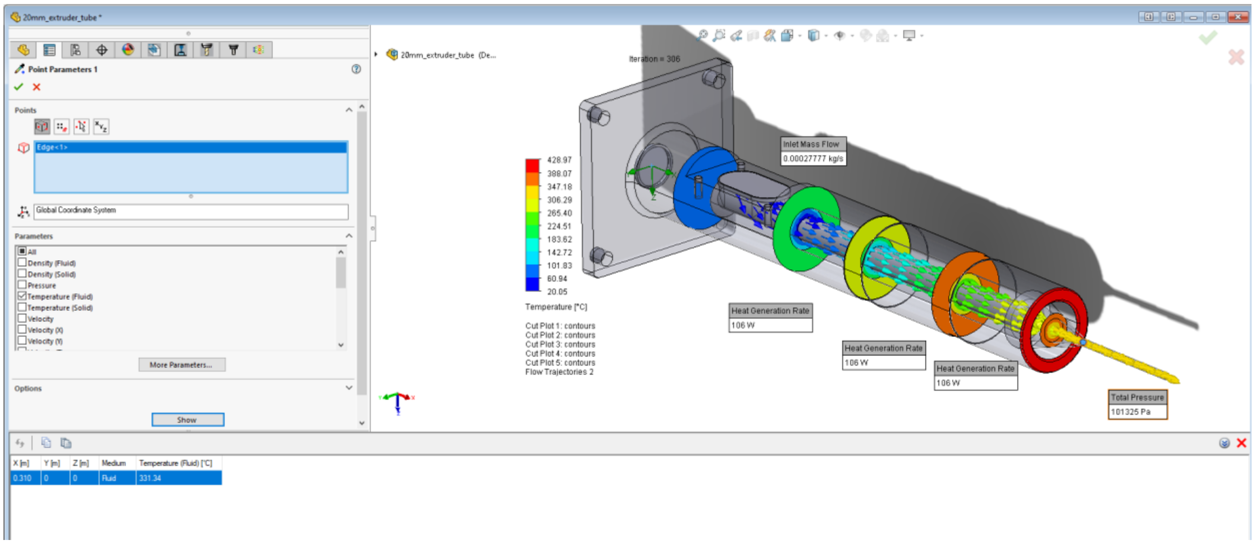

X [m]	Y [m]	Z [m]	Medium	Temperature (Fluid) [°C]
0.310	0	0	Fluid	331.34

Figure 10: Mesh Refinement of 4, Overall Results plus Nozzle Exit Temperature

(Nozzle exit temperature is 331C)

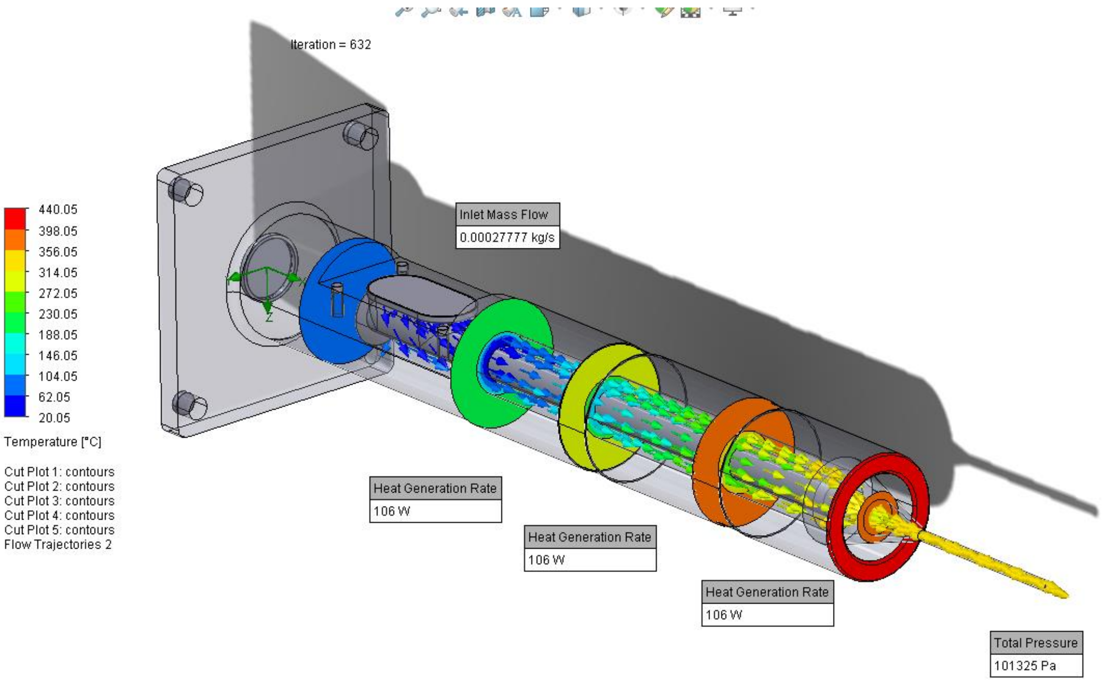

Figure 11: Mesh Refinement of 7, Overall Results

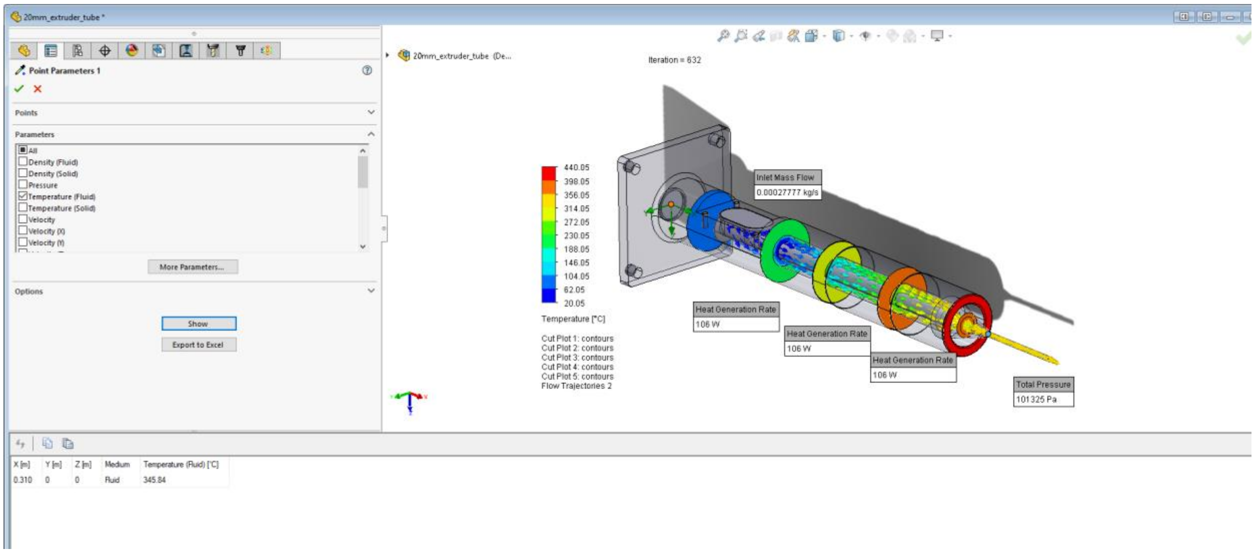

Point Parameters 1

Parameters

■ All
☐ Density (Fluid)
☐ Density (Solid)
☐ Pressure
☑ Temperature (Fluid)
☐ Temperature (Solid)
☐ Velocity
☐ Velocity (X)
☐ Velocity (Y)

Iteration = 632

Inlet Mass Flow: 0.00027777 kg/s

Heat Generation Rate: 106 W

Heat Generation Rate: 106 W

Heat Generation Rate: 106 W

Total Pressure: 101325 Pa

X [m]	Y [m]	Z [m]	Medium	Temperature (Fluid) [°C]
0.310	0	0	Fluid	345.84

Figure 12: Mesh Refinement of 7, Overall Results plus Nozzle Exit Temperature

(Nozzle exit temperature is 346C)

The difference between the two solution methods is only 15C, or a 4% difference. This indicates not only the result's independence of the mesh size, but also that a mesh refinement level of 4 is adequate for further computations. In addition, at the mesh refinement level of 7, the percent error in the nozzle exit temperature between the CFD simulation and the energy balance method is only 1%. This ensures the correctness of both the CFD simulation as well as the energy balance method. With an agreement between solution methods established and an adequate mesh refinement level determined (a level of 4 was selected due to the large difference in computation time and relatively small error) , further testing could be done to see how varying the energy input into each heating element affects the temperature distribution in the fluid, extruding barrel, and nozzle exit temperature. Multiple different heater input rates and combinations were considered, differentiated from one another by configuration number (note that the sum of the heat inputs are identical and equivalent to both the initial simulation as well as the energy balance method). Figures 13-24 indicate these results. Further note that configurations were split into A and B, with B also being inclusive of an average temperature at the nozzle exit.

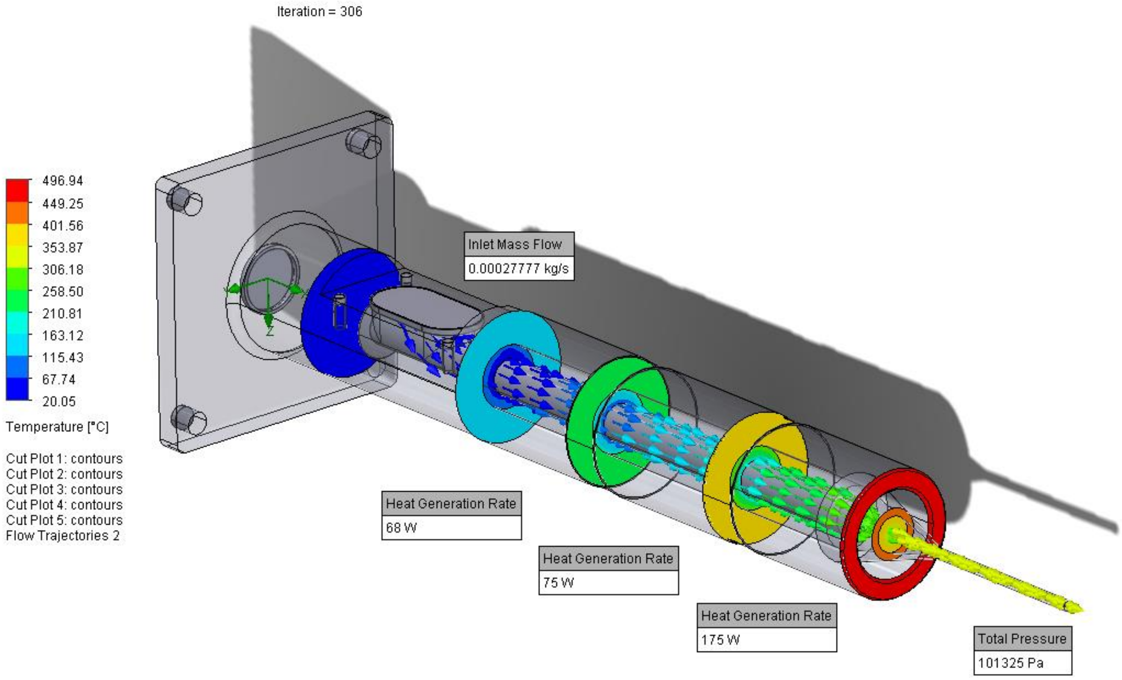

Figure 13: Configuration 1, Part A

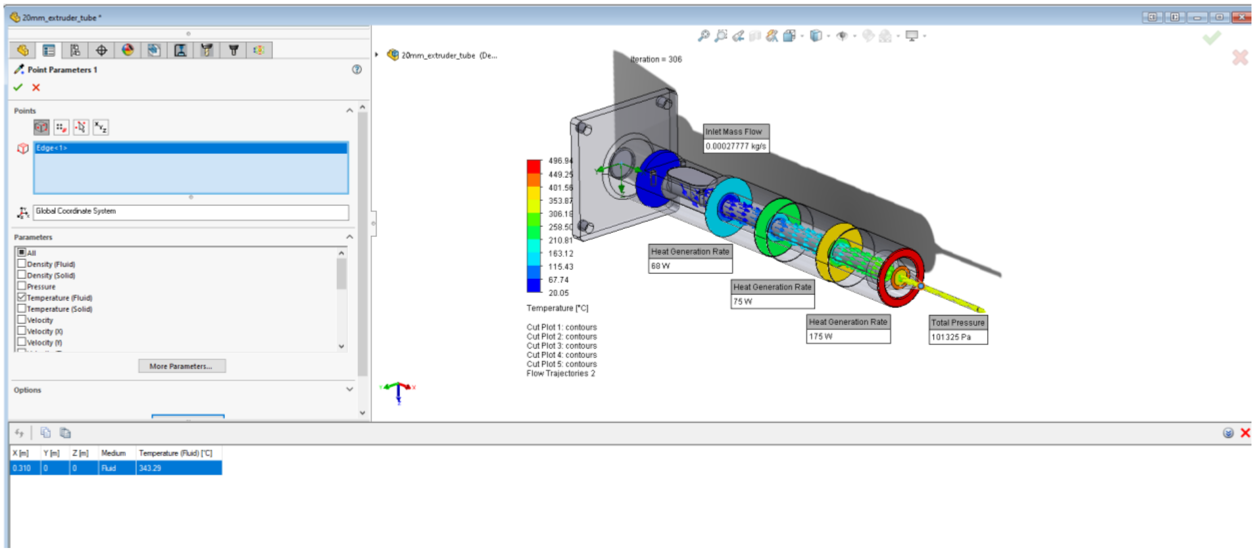

Edge<1>

Global Coordinate System

- ■ All
- ☐ Density (Fluid)
- ☐ Density (Solid)
- ☐ Pressure
- ☑ Temperature (Fluid)
- ☐ Temperature (Solid)
- ☐ Velocity
- ☐ Velocity (X)
- ☐ Velocity (Y)

X [m]	Y [m]	Z [m]	Medium	Temperature (Fluid) [°C]
0.310	0	0	Fluid	343.29

Figure 14: Configuration 1, Part B

(343C)

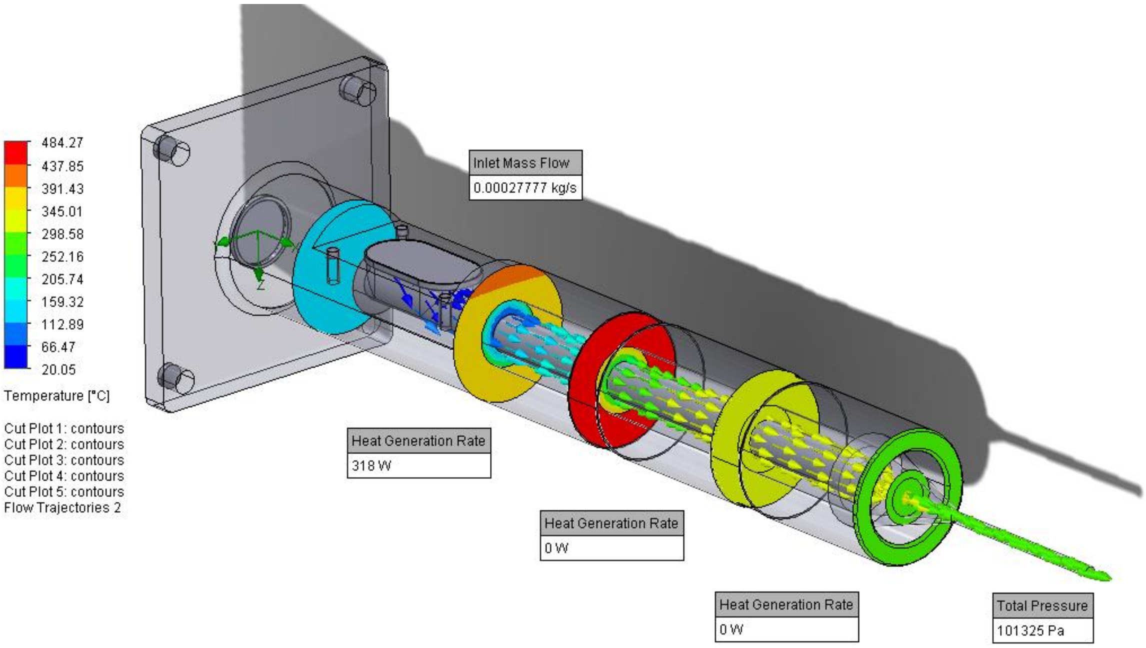

Figure 15: Configuration 2, Part A

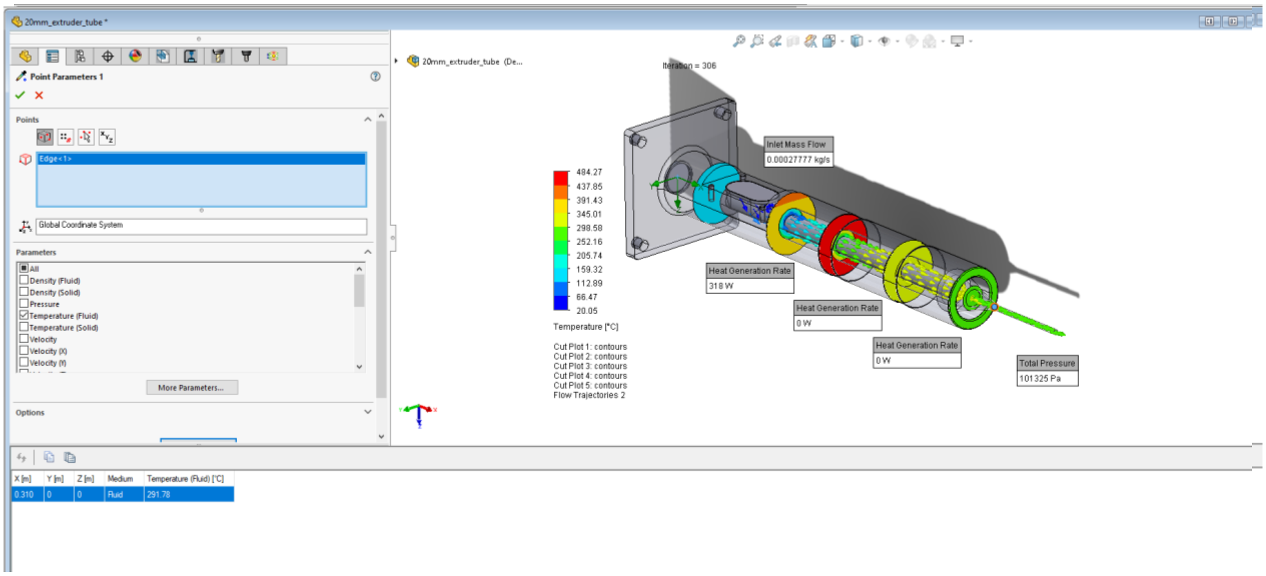

Edge<1>

Global Coordinate System

■ All
☐ Density (Fluid)
☐ Density (Solid)
☐ Pressure
☑ Temperature (Fluid)
☐ Temperature (Solid)
☐ Velocity
☐ Velocity (X)
☐ Velocity (Y)

X [m]	Y [m]	Z [m]	Medium	Temperature (Fluid) [°C]
0.310	0	0	Fluid	291.78

Figure 16: Configuration 2, Part B

(292C)

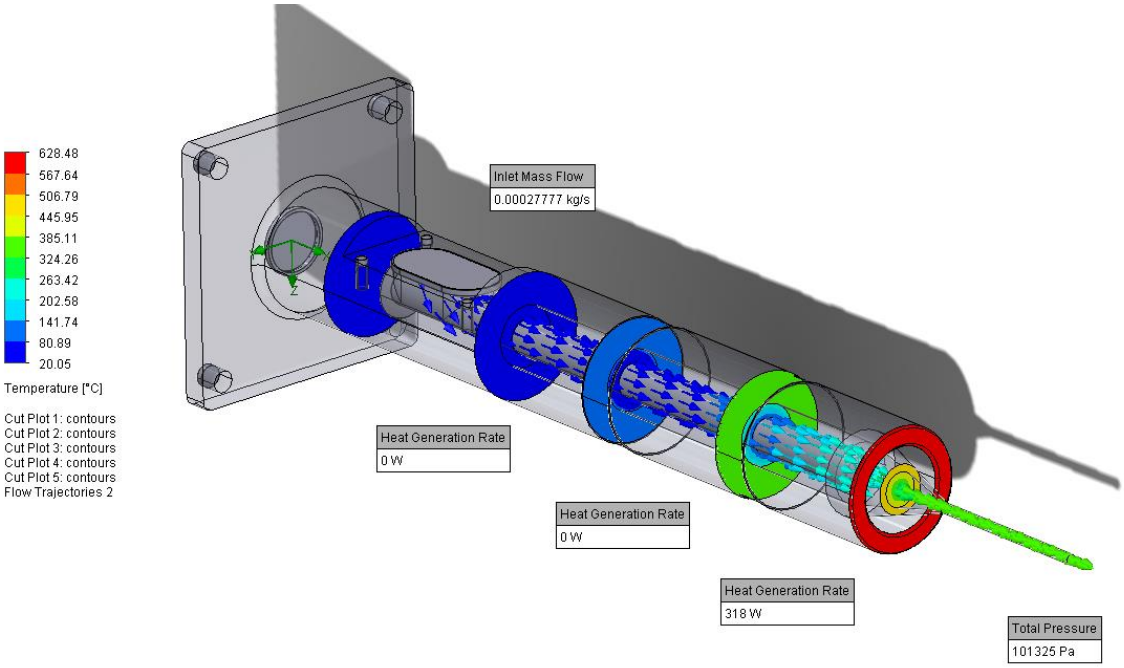

Figure 17: Configuration 3, Part A

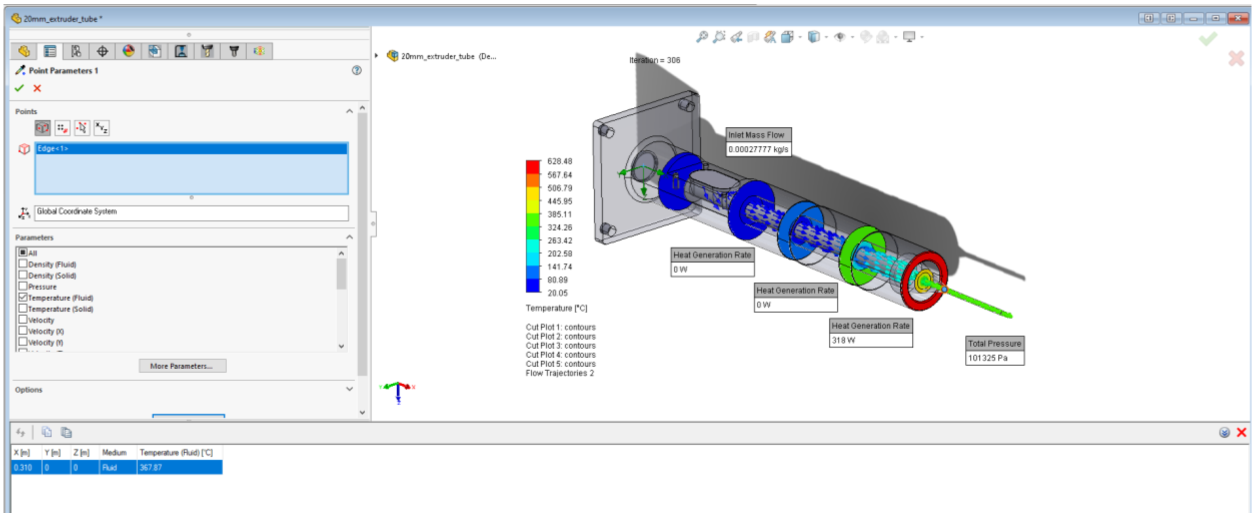

Edge<1>

Global Coordinate System

■ All
☐ Density (Fluid)
☐ Density (Solid)
☐ Pressure
☑ Temperature (Fluid)
☐ Temperature (Solid)
☐ Velocity
☐ Velocity (X)
☐ Velocity (Y)

X [m]	Y [m]	Z [m]	Medium	Temperature (Fluid) [°C]
0.310	0	0	Fluid	367.87

Figure 18: Configuration 3, Part B

(367 C)

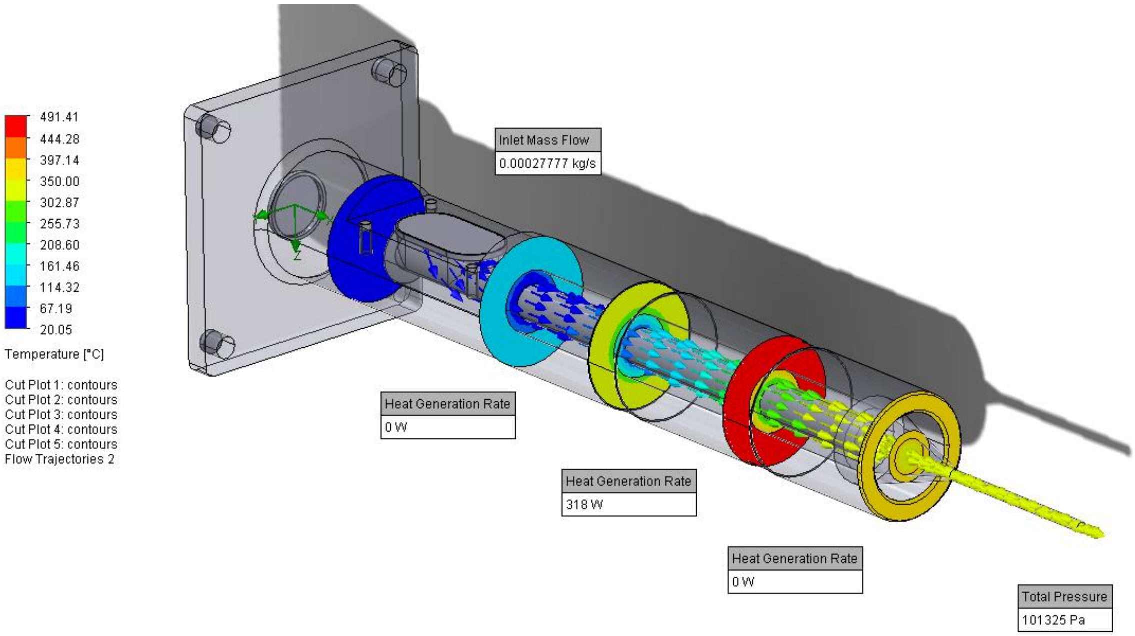

Figure 19: Configuration 4, Part A

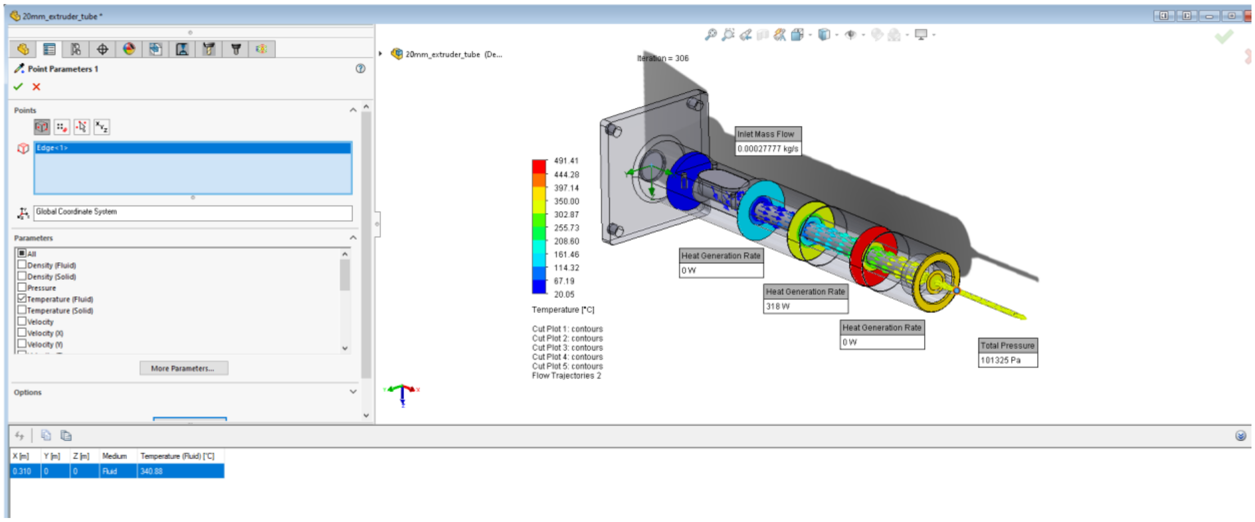

Global Coordinate System

■ All
☐ Density (Fluid)
☐ Density (Solid)
☐ Pressure
☑ Temperature (Fluid)
☐ Temperature (Solid)
☐ Velocity
☐ Velocity (X)
☐ Velocity (Y)

X [m]	Y [m]	Z [m]	Medium	Temperature (Fluid) [°C]
0.310	0	0	Fluid	340.88

Figure 20: Configuration 4, Part B

(341C)

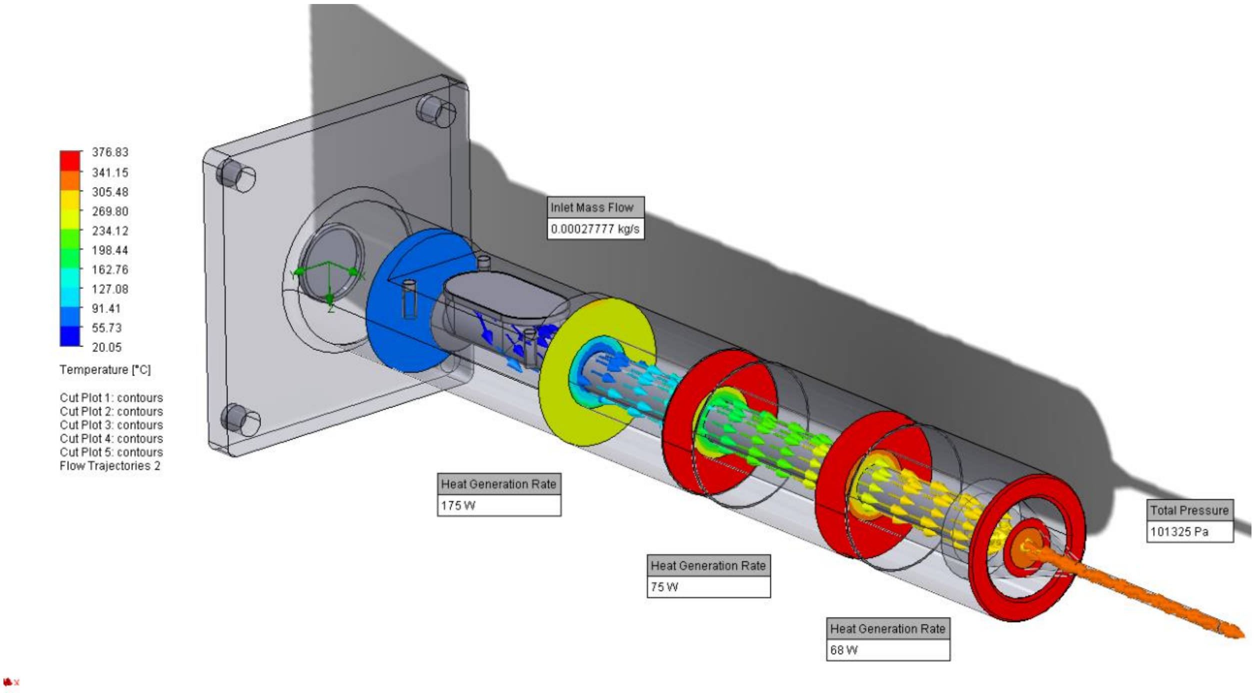

Figure 21: Configuration 5, Part A

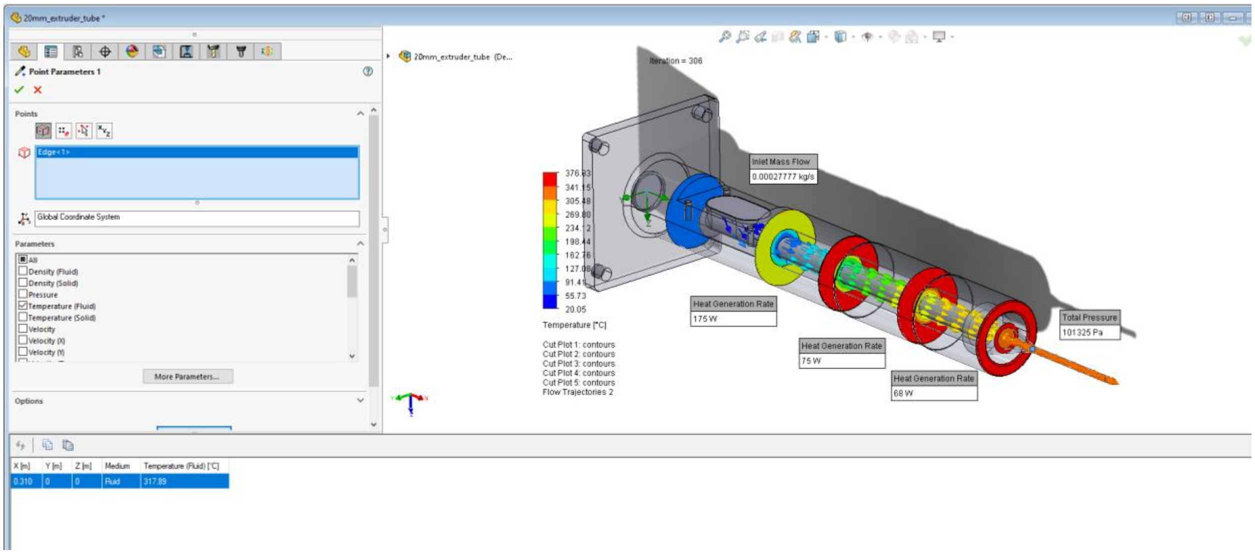

Edge<1>

Global Coordinate System

☑ Temperature (Fluid)

X [m]	Y [m]	Z [m]	Medium	Temperature (Fluid) [°C]
0.310	0	0	Fluid	317.89

Figure 22: Configuration 5, Part B

(318C)

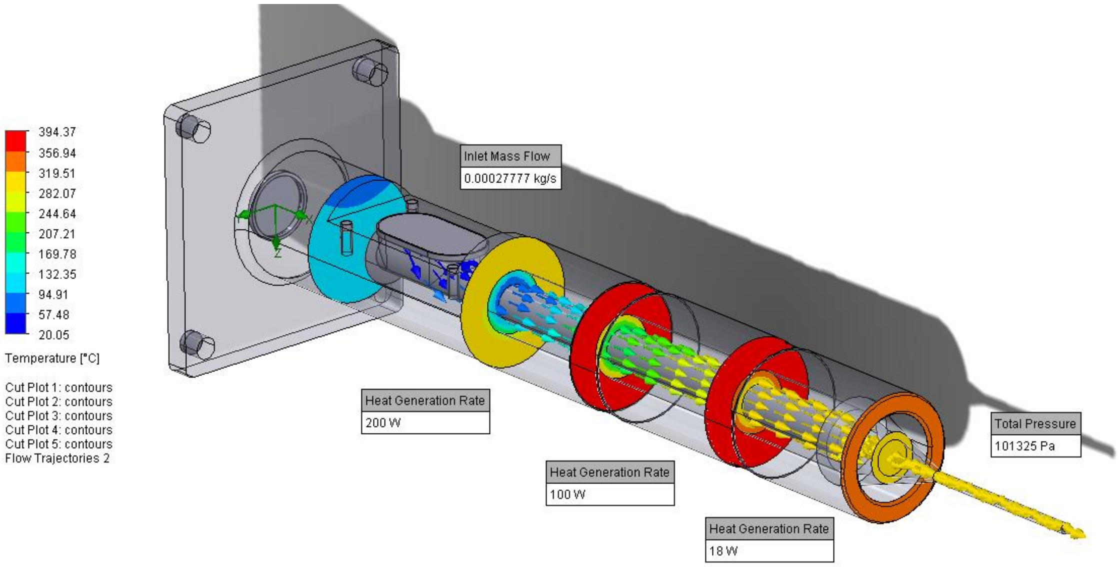

Figure 23: Configuration 6, Part A

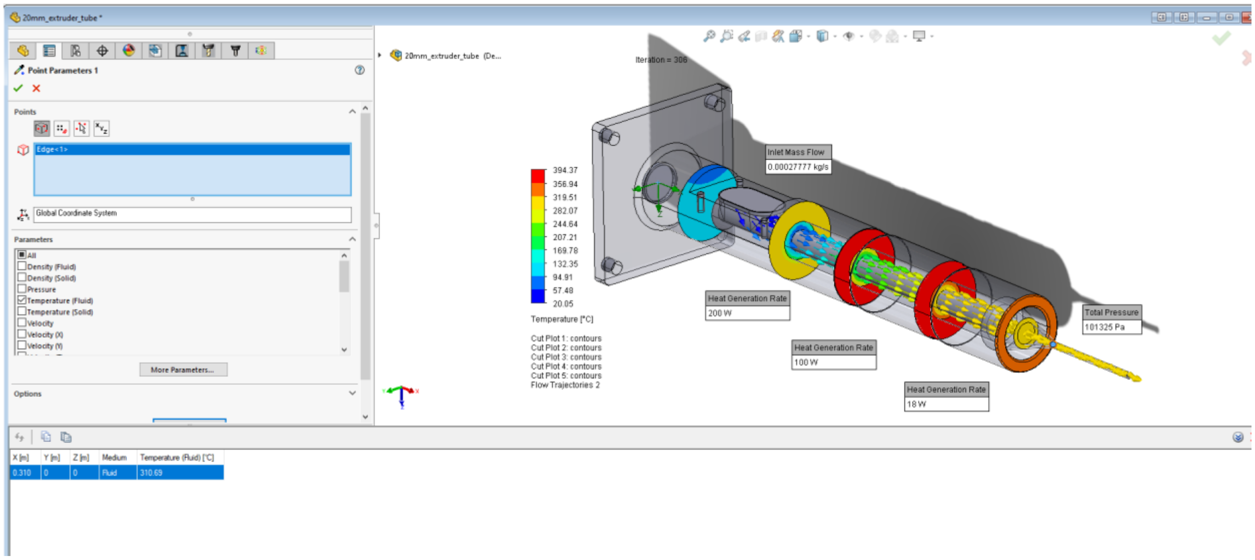

Edge<1>

Global Coordinate System

Parameters

- ■ All
- ☐ Density (Fluid)
- ☐ Density (Solid)
- ☐ Pressure
- ☑ Temperature (Fluid)
- ☐ Temperature (Solid)
- ☐ Velocity
- ☐ Velocity (X)
- ☐ Velocity (Y)

X [m]	Y [m]	Z [m]	Medium	Temperature (Fluid) [°C]
0.310	0	0	Fluid	310.69

Figure 24: Configuration 6, Part B

(310C)

By reviewing Figures 13-24, it is evident that the allocation of heat for each heating element affects the temperature distribution in the barrel, the fluid, and the nozzle exit temperature. Depending upon which temperature distribution is deemed to be most critical, different optimum heater input allocations can be determined. Deciding on an optimum heater input allocation will likely require experimental testing, but based on the configurations considered, a general trend can be determined. When the majority of the heat input is nearest the material entry point, the temperature distribution inside of the extruding barrel remains the most constant. In addition, this would help to ensure that the solid input material is rapidly transformed into a liquid to allow easy passage throughout the remainder of the extruding barrel. At this point in the design process (3/19/21), allocating the majority of the heat input nearest the material entry point and doing fine tuning at the nozzle seems to be the best configuration.